A heat-powered ejector chiller working with low-GWP fluid R1233zd(E) (Part 1: Experimental results)

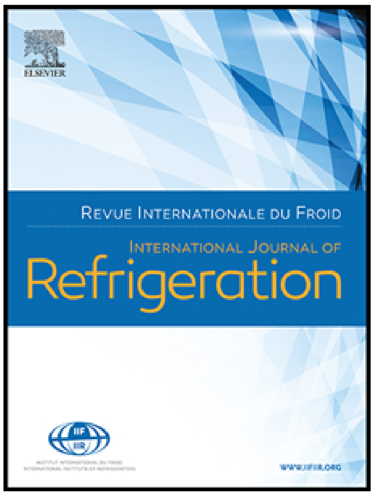

A heat-powered ejector chiller working with low-GWP fluid R1233zd(E) (Part 1: Experimental results)

Jafar Mahmoudian , Andrea Rocchetti , Federico Mazzelli , Adriano Milazzo

PII: S0140-7007(20)30425-4
DOI: https://doi.org/10.1016/j.ijrefrig.2020.10.015
Reference: JIJR 4927

To appear in: *International Journal of Refrigeration*

Received date: 19 February 2020
Revised date: 19 July 2020
Accepted date: 12 October 2020

A heat-powered ejector chiller working with low-GWP fluid R1233zd(E)

(Part 1: Experimental results)

Jafar Mahmoudian, Andrea Rocchetti, Federico Mazzelli, Adriano Milazzo[*]

DIEF- Department of Industrial Engineering, University of Florence – via S.Marta, 3, 50139 Florence (ITALY)

[*]Corresponding author: adriano.milazzo@unifi.it

Abstract

A prototype ejector chiller with nominal cooling power of 40 kW, designed according to the “CRMC” criterion, has been tested by our research group since 2011. The prototype has undergone several refinements and finally has been upgraded to R1233zd(E), which is non-flammable, has low-GWP and favourable thermodynamic properties, i.e. “dry-expansion” and moderate pressure at generator. In terms of saturation pressure curve, the new fluid is similar to R245fa, which was previously used in the prototype. Hence, R1233zd(E) has been basically used as a “drop-in” replacement. The ejector chiller was tested at different evaporation temperatures (2.5 to 10°C), typical of air conditioning applications. Saturation temperatures at generator from 95 to 105°C have been selected as representative of waste-heat recovery. The experimental findings prove that the CRMC ejector has a satisfactory performance with the new working fluid.

Keywords: Ejector chiller, CRMC, R1233zd(E), Experimental method, Drop-in low-GWP fluid.

Nomenclature			
h	Specific enthalpy, kJ kg^{-1}	G	Generator
$\dot{m}$	Mass flow rate, kg s^{-1}	m	Motive or primary flow
P	Pressure [bar, MPa]	out	Outlet
$\dot{Q}$	Heat flux, W	pump	Referred to pump
T	Temperature, [°K, °C]	s	Secondary flow
$\dot{W}$	Power input, W	sat	Saturation
		w	Water side at the heat exchanger
Subscripts		Acronyms	
C	Condenser	ER	Entrainment Ratio
E	Evaporator	COP	Coefficient Of Performance
		GWP	Global Warming Potential

1. Introduction

Heat driven refrigeration plays a crucial role among the many options for waste heat recovery. Currently, the most successful technology for heat driven refrigeration is undoubtedly absorption. Alternative technologies are actively sought, but none of them seems a clear winner. Low cost, efficiency, flexibility and robustness are the most important issues for any competing technology. Ejector refrigeration may be promising under some of these respects and has been the main research topic of our research group since many years.

The idea of using ejectors to produce vacuum and hence low-temperature evaporation of water in order to perform a cooling effect is commonly credited to Maurice Leblanc [1] and dates back to the first decade of the 20th century. Specific advantages of ejector refrigerators are mechanical simplicity, ability to work with ‘‘environmental friendly’’ refrigerants, low investment cost and relatively high efficiency in comparison with other heat operated refrigerators [2]. A detailed account of heat-driven ejector refrigeration system analysis, design and operation is presented in [3]. A comprehensive review of studies has been offered in [4] and more recently in [5]. A discussion of the interaction between component and system efficiency is presented in [6].

Ejector refrigeration cycles replace the mechanical compressor by a liquid feed-pump, a vapour generator and a supersonic ejector. The ratio between cooling load and total heat and power inputs yields the Coefficient Of Performance (COP), which summarizes the system performance:

$$COP = \frac{\dot{Q}_E}{\dot{Q}_G + \dot{W}_{pump}} = \frac{\dot{m}_s}{\dot{m}_m} \frac{\Delta h_E}{(\Delta h_G + \Delta h_{pump})}$$

The ratio of entrained (secondary) to motive (primary) mass flow rate defines the Entrainment Ratio:

$$ER = \frac{\dot{m}_s}{\dot{m}_m}$$

Entrainment ratio (ER) is maximized when the mixed flow in the mixing chamber reaches supersonic speed, so that the quantity of entrained suction flow is independent of the discharge pressure. This operation mode is called "on-design" or in "chocked regime". Conversely, the amount of suction flow drawn into the ejector depends on the outlet pressure when the secondary flow is subsonic and the operation is said to be "off-design". The value of discharge pressure separating these two operation zones is called "critical pressure" and, once translated in a condensation temperature, qualifies the ability of an ejector chiller to operate at a given ambient temperature.

A largely debated topic in the discussion about ejector chillers is the choice of the working fluid. R245fa, successfully used by our group ([7] [8]) and many others ([9] [10]), is still investigated in the refrigeration arena by some researchers [11] [12], but has a very high GWP = 950. Milazzo and Rocchetti [13] compared several alternative fluids, using a thermodynamic model accounting for real gas properties and adapting the ejector geometry to each gas by the CRMC criterion. Following the outcome of this study, we concentrated on R1233zd(E), a "dry expansion fluid" (i.e. featuring an inward slope of the upper limit curve on the temperature – entropy diagram) with 204.9 kJ/kg latent heat and 2.82 kg/m^3 vapour density, i.e. similar thermodynamic properties to R245fa. On the other hand, R1233zd(E) has very low GWP (around 1) [14] and is not flammable. R1233zd(E) was considered as a replacement for R245fa also in [15] and [16].

To the best of our knowledge, the experimental data reported within this paper are the first published on the use of R1233zd(E) within an ejector chiller, a part from a few preliminary results presented in 2019 by the same authors [17]. Even if our group is strongly committed to the diffusion of "natural" refrigerants, the availability of a non-flammable, non-toxic and low-GWP fluid could indeed open interesting opportunities. With respect to steam, R1233zd(E) offers a much higher volumetric refrigeration capacity and is able to reach sub-zero temperatures. This gives a plus with respect to steam ejector chillers and lithium-bromide absorption chillers. With respect to other low-GWP fluids, R1233zd(E) allows to build an ejector chiller featuring a lower generator pressure for a given waste-heat source temperature, reducing the energy expenditure and cost of the feed pump.

Once further optimized in terms of COP and critical pressure, the ejector chiller working with R1233zd(E) would offer a reliable, compact, economic, F-gas compliant heat-powered refrigeration system, able to reach sub-zero temperature. At favorable working conditions, the chiller could even use an air-cooled condenser. Last but not least, such chiller would avoid the problems of solution crystallization that affect lithium-bromide absorption chillers.

2. Experimental apparatus

2.1. General view

Our prototype heat-powered refrigeration system (Figure 1) was designed to give 40 kW of cooling power to chilled water entering at 12°C and exiting at 7°C. A vertical layout saves floor-space and guarantees a substantial liquid head between the condenser (on top) and the generator feed-pump (on the bottom). This latter is a multi-stage side-channel pump, (Speck Pumpen SK 20), featuring a good resistance to cavitation and a magnetic coupling between the electric motor and the pump, in order to avoid any fluid leakage. An inverter allows to vary the rotation speed of the pump, but the test presented herein have been all carried on at 50 Hz frequency. The pump has not been specifically selected for its energy efficiency, but rather aiming at maximum flexibility and robustness in view of an experimental activity. Whenever this prototype will evolve into a practical chiller, the energy consumption, cost and durability of the pump (the sole moving part of the chiller) will need a careful optimization.

A thermal oil electric heater is used as heat source, while an evaporative cooling tower discharges the system power into the ambient air outside the laboratory. The cooling tower receives the warm water directly from the condenser and feeds a buffer tank that guarantees a thermally stable water source at near ambient temperature. The tank water is used to give the heat load to the evaporator and to cool the condenser. By-pass branches are used to regulate the temperature at evaporator and condenser inlets (Figure 2).

Heat exchangers are all stainless steel, brazed plate, commercial units. Generator and evaporator are carefully insulated, while the condenser is not, given that it works at near-ambient temperature. The fluid circuit, comprising D=100 mm stainless steel gas-carrying tubes and D=40 mm copper tubes for liquid, is fully insulated as well (some parts of the insulation are removed in Fig. 1). The ejector is visible on the upper left side of Fig 1a and will be discussed in detail in the next section. The long vertical pipe that connects the condenser to the electronic expansion valve acts as a liquid receiver, guaranteeing uninterrupted liquid feed to the valve during transients.

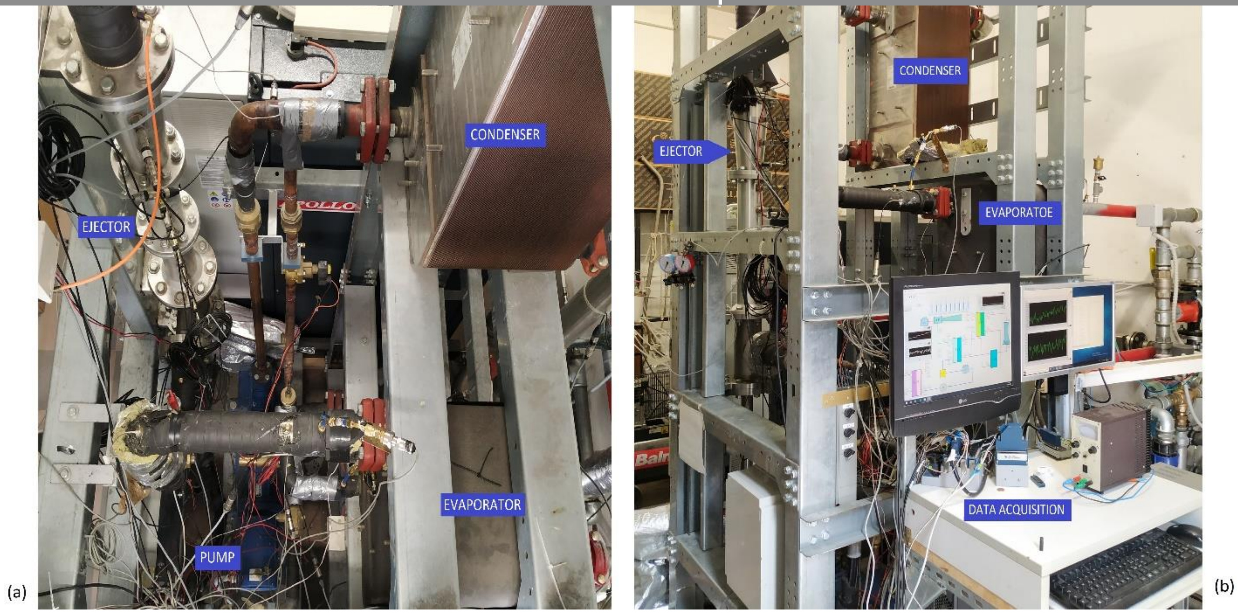

Figure 1 – Top (a) and side (b) views of prototype

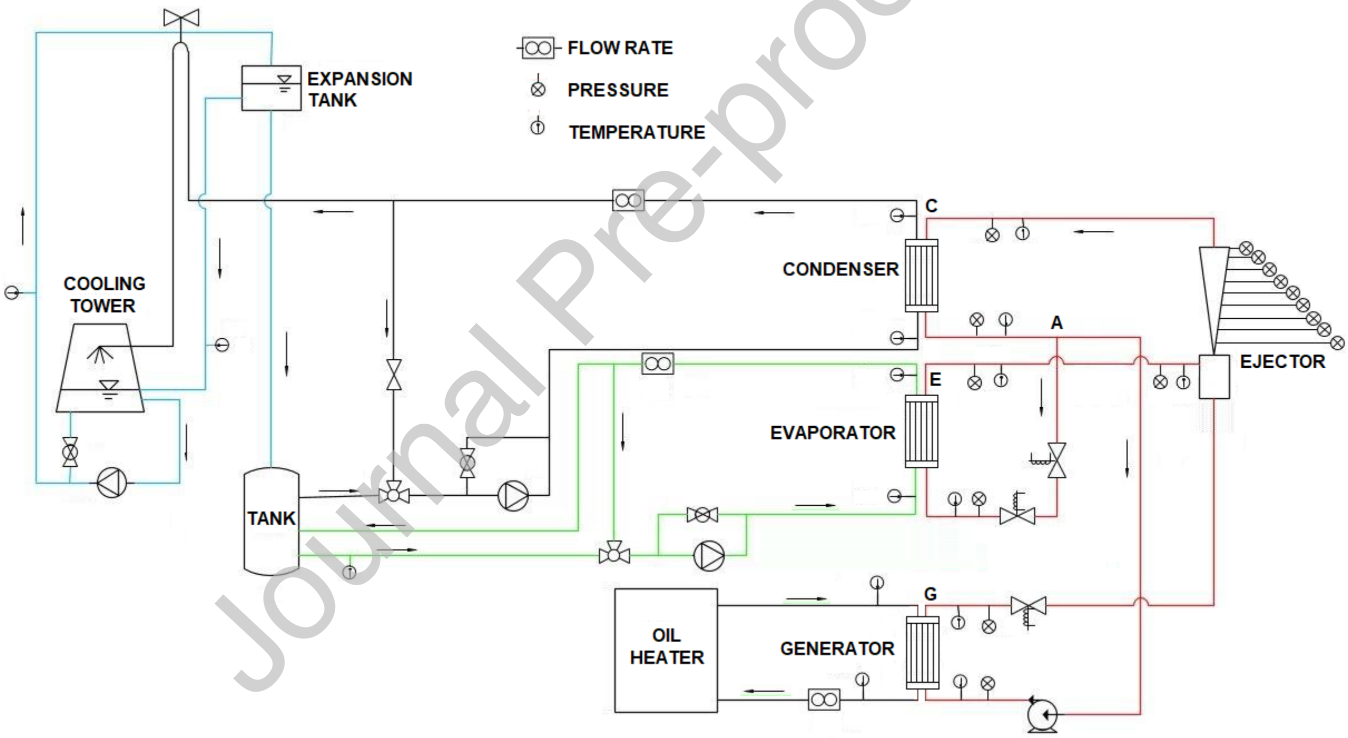

Figure 2 – Experimental setup

2.2. Ejector design

As shown in fig. 3, the ejector features a bell shaped inlet on the suction side and a conical outlet on the discharge side. In between, the duct is shaped according to the CRMC (Constant Rate of Momentum Charge) criterion introduced in 2002 by Ian Eames [18]. The profile generated by the CRMC criterion has a continuous curvature (even if the departure from a straight cylinder is rather small). This profile may be easily optimized by setting the rate of momentum change, which dictates the length of the diffuser. The benefit in terms of efficiency, either in terms of entrainment ratio or compression ratio have been shown in [19]. Recently Kitrattana *et al* [20] reported a comparison between a CRMC and a conventional steam ejector in the same conditions and found that the CRMC has a 40% higher entrainment ratio.

The manufacturing problems due to the small inner diameter and substantial length forced to build the ejector in three pieces, carefully aligned by flanged connections. This issue is due to the relatively small cooling power of our

prot[illegible]ed manufacturing techniques.
The present chiller is the result of a long refinement work, from a very first design in 2011 [21] to present configuration, extensively described in [7]. Main geometrical data of the ejector in the present configuration are reported in Table 1.
The ejector features 9 ports drilled perpendicularly to the internal profile, placed at 100 mm intervals and starting at 50 mm from the inlet flange of the ejector, as shown in Figure 3. The primary nozzle can be moved forward and backward from a reference position having the nozzle exit plane coincident with the inlet plane of the suction chamber. All data presented herein have been obtained with the nozzle in the reference position.

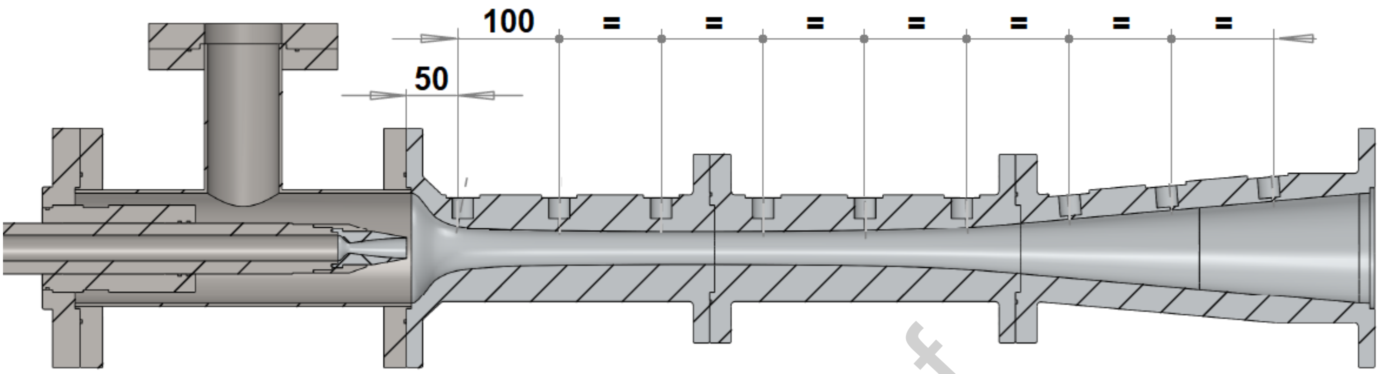

Figure 3 – CRMC ejector with static pressure ports and movable primary nozzle

	Nozzle	Diffuser
Throat diameter [mm]	10.2	31.8
Exit diameter [mm]	20.2	108.3
Length [mm]	66.4	950
Material	Aluminium	Aluminium

Table 1– Main geometrical parameters of the ejector

2.3. Measuring sensors & data acquisition

Mass flow meters and temperature sensors are mounted on the condenser and evaporator water circuits, in order to have the instantaneous energy balance of the system. Temperature and pressure sensors are mounted in all the significant points along the refrigerant circuit, while 9 static pressure probes are mounted along the ejector as above mentioned. The specifications of the main sensors are reported in Table 2. LABVIEW 2014 software is used to acquire the signal from the sensors and calculate in real time some control parameters.

Instrument	Model/type	Position	ADC Module	Total uncertainty
Piezoresistive pressure transducer	PA25HTT 0-30 bar	Diffuser	NI9208	±(0.1% + 0.22% FS)
	PR23R 0.5-5 bar	Evaporator	NI9208	±(0.1% + 0.22% FS)
	PA21Y 0-30 bar	Generator, Condenser	NI9208	±(0.08% + 1.0% FS)
Resistance temperature detector	Pt100	Whole Plant	NI9216, NI9217	±0.25°C
Thermocouple	T	Whole Plant, Cooling Tower, Tank	NI9213	±1.0°C
Electromagnetic water flowmeters	Endress Hauser Promag 50P	Condenser	NI9219	±(0.5% + 0.04% FS)
Compact Rotamass	YOKOGAWA	Evaporator	NI9219	±(0.05% + 0.1% FS)

Vortex flowmeter	YOKOGAWA YF105	Generator	NI9219	±(0.8% + 0.1% FS)

Table 2– Specifications of the transducers and data acquisition modules

"Multiple sample" uncertainty analysis [22] [23] has been applied for this work. All data are acquired every second. All uncertainties are evaluated with a confidence level of 95%. Bias errors are calculated by summing up the contributions stated by the manufacturers for both the instruments and data acquisition system. More details on the procedure are described by Mazzelli *et al* [7]. The total absolute uncertainty of the ER in experimental tests is around 5%. This uncertainty can be explained considering that ER is calculated from evaporator and condenser powers (measured on the hydraulic side) and the pressure transducers have a large measuring range due to the initial specifications of the prototype, which was intended to host different working fluids. Unfortunately, the compact design of the prototype does not allow the installation of two suitable mass-flow meters on the refrigerant circuit. It's worth remembering that mass flow meters are themselves bulky and require long straight pipes up and downstream, in order to give a reliable measurement. Therefore, for now, we must rely on indirect measuring. An evaluation of the heat transfer towards the environment has been performed and the results show that, given the high cooling power of the prototype, this issue should cause a tolerable error.

3. Results and discussion

All saturation temperatures reported below are calculated via NIST REFPROP functions [24] from the pressure measured on top of each heat exchanger. The experiments presented herein are referred to saturation temperatures of 97°C and 103°C at the generator. Saturation temperature at evaporator is varied from 2.5°C to 10 °C.
During each test run, condensation temperature is increased in small steps (e.g. 0.5°C) by means of a 3-way valve that controls a by-pass on the cooling water circuit. Generator and evaporator saturation temperatures are kept at fixed values. When stable operation is attained, the experimental point is taken as an average over at least 3 minutes. The electronic expansion valve is manually operated, in order to fix the saturation temperature at the evaporator without undue oscillations introduced by any control system. As the condenser pressure is increased to a certain level, the cooling power reduces to zero and the experiment is stopped, in order to avoid backflow from the condenser to the evaporator.
Chilled water temperature drop across the evaporator is kept fixed at 5°C, by modulation of the water flow rate. Outlet water temperature is at least 2.5°C higher than the evaporator saturation temperature throughout the test campaign. Therefore, inlet water temperature is generally 7-8 °C higher than evaporator saturation temperature. This causes a high superheating at evaporator exit, especially at low evaporation temperature, and hence a low vapour density at secondary inlet, i.e. a reduced entrainment ratio and COP. On the other hand, the relatively high water temperature avoids any risk of icing. Obviously, this restriction could be overcome if a suitable anti-freeze were added to the chilled water, improving the COP and making operation at sub-zero temperature readily feasible.
The eight different performance curves in Figure 4 show the well-known behaviour of supersonic ejector chillers, featuring increasing COP and critical condensation temperature with increasing saturation temperature at evaporator, while the saturation temperature at generator has a favourable effect on the critical condenser pressure, but a negative effect on the COP. In the case of generator saturation temperature T_G = 103°C (four curves on the right), the ejector chiller can work with rather high condensation temperature. For example, at 10°C evaporation temperature (suitable e.g. for air conditioning), the critical saturation temperature at the condenser is 35.5°C, allowing operation with an air-cooled condenser, at least in mild climates.
The slope of the off-design line shows a decrease as the evaporation temperature increases. In other words, the off-design condition takes place in a more gradual way, with relatively stable, though deteriorated, operation even at condenser temperature significantly above the critical value. At lower evaporator temperature the off-design lines are much steeper.
When the generator temperature is lowered to T_G = 97°C (four curves on the left), the nozzle accommodates a lower amount of primary flow, while the secondary flow is entrained at roughly the same rate, so that entrainment ratio and COP are higher. On the other side, at lower generator temperature the ejector critical back pressure reduces i.e. the ejector moves to off-design at lower temperature.

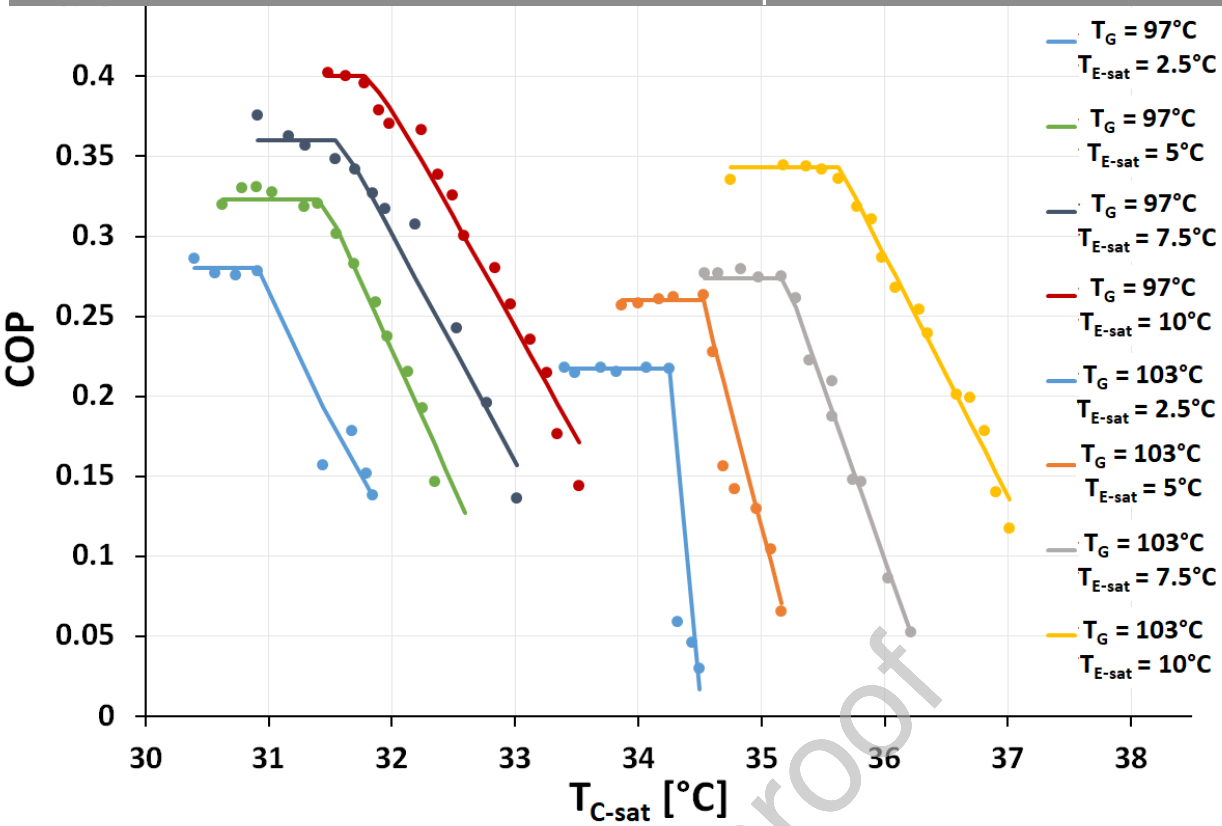

Figure 4 – Experimental COP of the chiller in different conditions

A more detailed description of the ejector operation may be gathered from the observation of the pressure profile along the ejector. The spacing between the transducers (100 mm – see Figure 3) does not allow a precise positioning of the shock train, but is sufficient to get a general picture and to discriminate between on and off-design working conditions[1]. For completeness, the readings of the pressure transducers at evaporator exit and at condenser inlet have been added.

At low evaporator saturation temperature (2.5°C), two shapes are clearly distinguishable in the pressure profiles: the curves from 1 to 4 in Figure 5 and from 1 to 6 in Figure 6 all show a common pressure values up to the transducer at 250 mm from the diffuser inlet. Given that the diffuser throat is located around 300 mm, the sharp pressure rise between 250 and 350 mm in these curves marks the transition between supersonic and subsonic flow.

The other curves in these two figures show a completely different shape, featuring a sharp pressure increases before 250 mm and then a slower increase before 550 mm, i.e. witnessing a fully off-design working condition. The COP v/s $T_{C\text{-}sat}$ graphs in the lower right corner of the figures locates the points corresponding to the various lines in the on or off-design zone. In Fig. 5, curve 4 may be taken as representative of the critical condition and is still fully on design. The intermediate condition between curves 4 and 5 was very unstable and was not recorded, while curve 5 is fully off design. In Fig. 6, on the other hand, curve 6 still gives an undiminished COP, but the pressure profile is already quite different from that of curve 5. This may explain the abrupt fall in COP registered at point 7.

[1] The lines connecting the points are drawn only as a visual aid and do not give any indication about the pressure between the sensors.

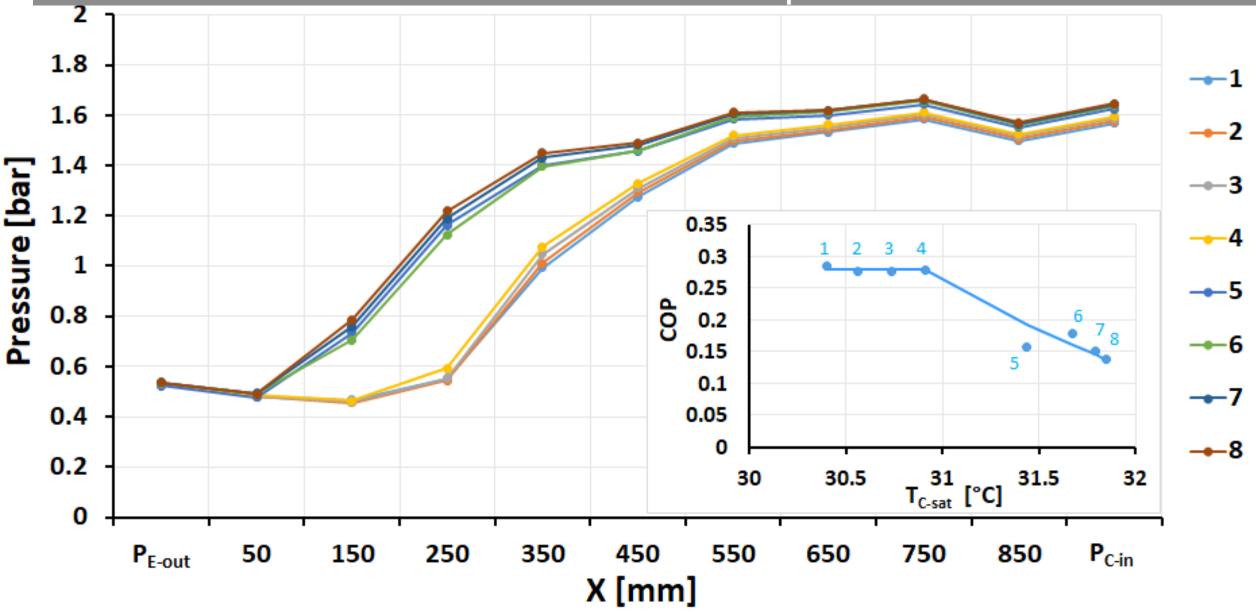

Figure 5 – Pressure values along the ejector T_G = 97°C, $T_{E\text{-}sat}$ = 2.5°C

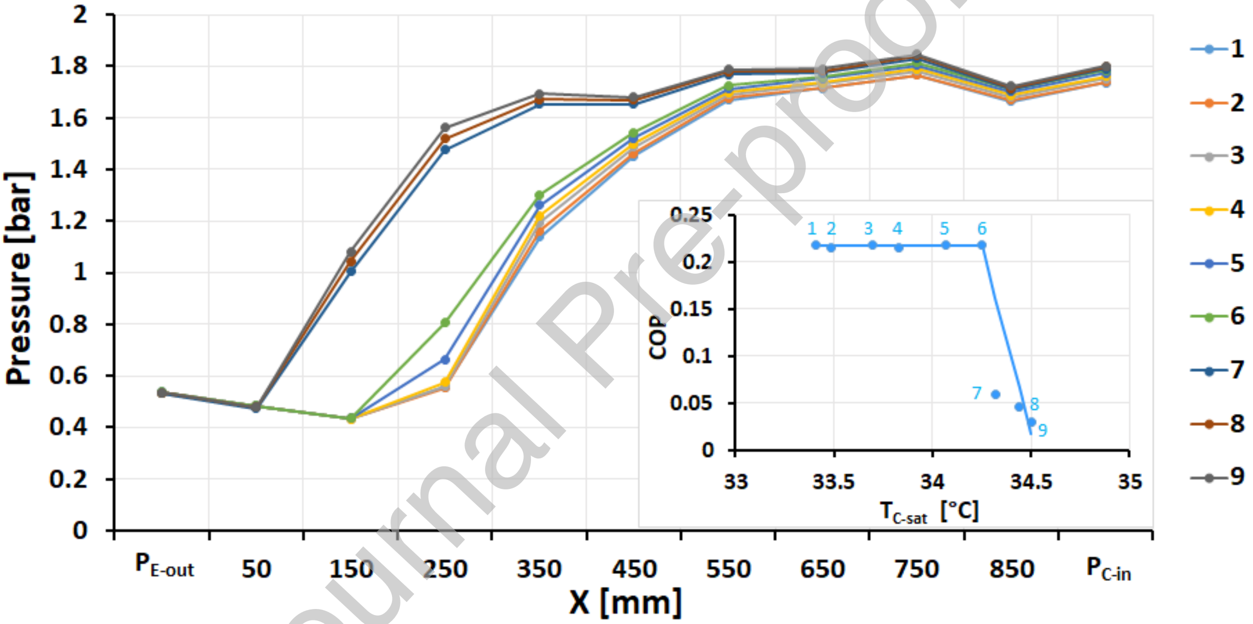

Figure 6 – Pressure values along the ejector T_G = 103°C, $T_{E\text{-}sat}$ = 2.5°C

Figure 7 and Figure 8, referred to 10°C saturation temperature at evaporator, show a completely different scenario with an almost continuous evolution of the pressure profile. Apparently, a first group of lines (1-3 in Fig. 7 and 1-4 in Fig. 8) has almost coincident pressures up to the second transducer (150 mm). However, the third transducer (250 mm) shows a wide range of pressures. This proves how imprecise is the common view of a normal shock taking place within the ejector in the on-design operation. In real operation the pressure oscillates along the ejector in a complex way and the boundary layer introduces a smoothing that complicates the analysis even further. Basically, from 200 mm onward we may say that the pressure profiles are equally distributed between the on-design and the extreme working condition (lines 15 in Figure 7 and line 16 in Figure 8), where cooling power is reduced to zero.

This explains the relatively slow rate of decrease registered by the COP when the critical point is overcome. In these conditions the ejector may be safely operated in the close vicinity of the critical point, because an accidental small increase of the condensation pressure would not cause a catastrophic failure.

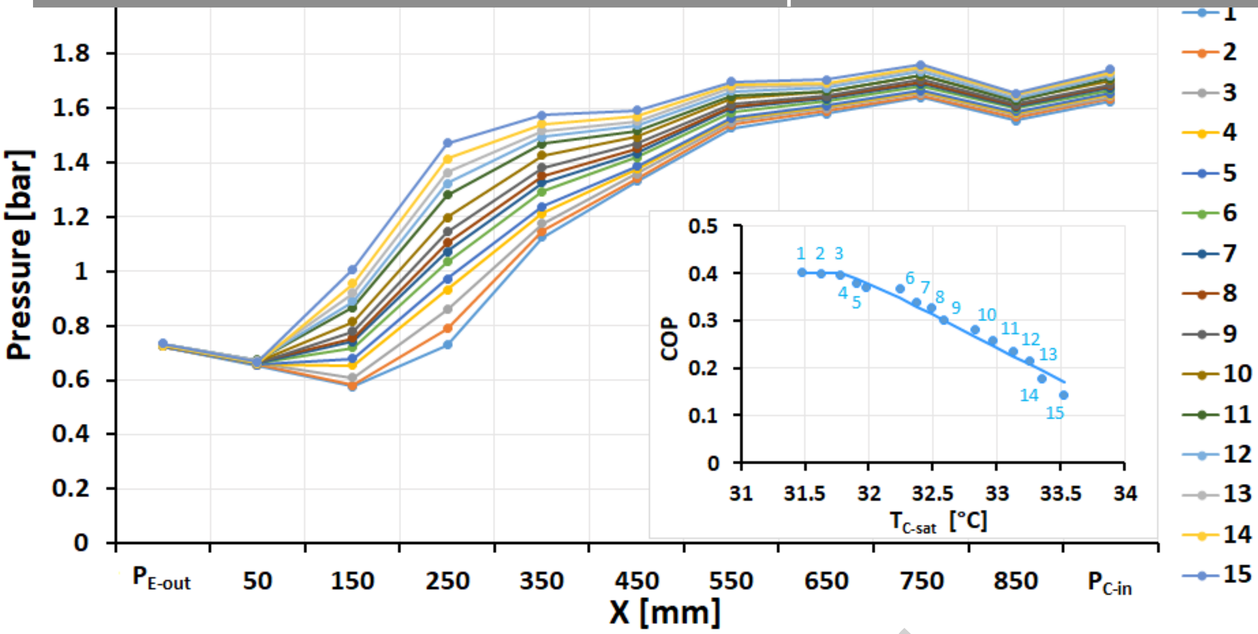

Figure 7 – Pressure values along the ejector T_G = 97°C, $T_{E\text{-}sat}$ = 10°C

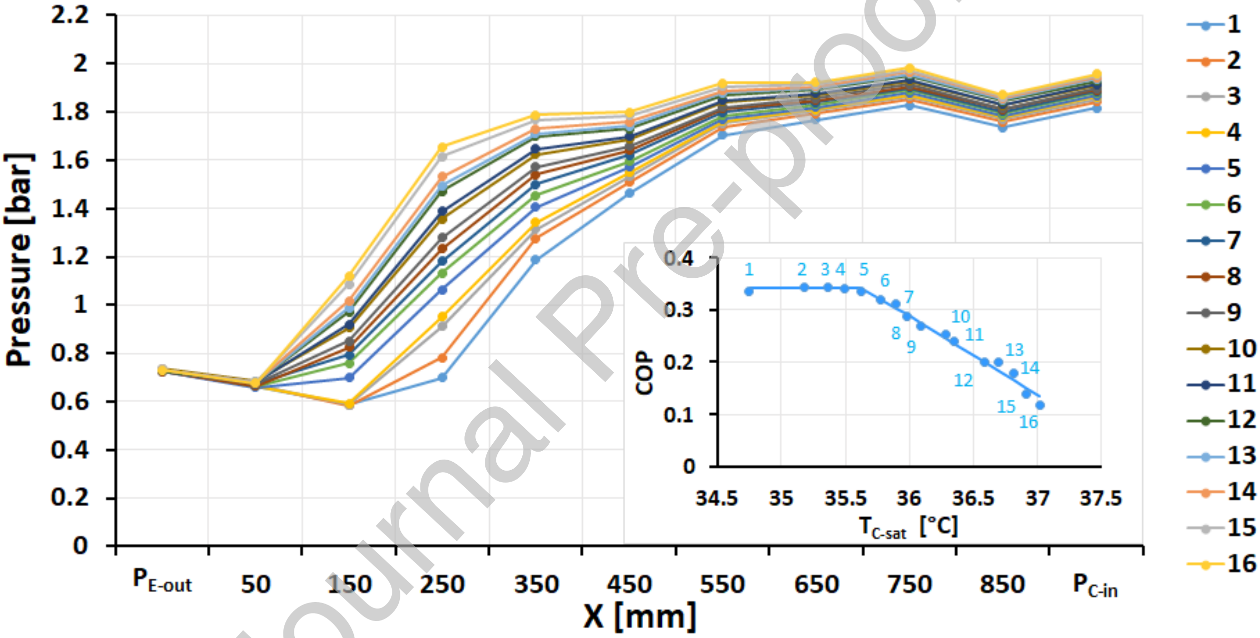

Figure 8 – Pressure values along the ejector T_G = 103°C, $T_{E\text{-}sat}$ = 10°C

All these graphs clearly show that the pressure recovery after 550 mm is null or even negative. A remarkable pressure reduction occurs between 800 mm to 900 mm. As anticipated, this is due to a poor design of the last part of the ejector, probably yielding a flow recirculation. The choice of truncating the CRMC profile and substituting its last part with a straight cone was taken in the early design process as a conservative measure, but apparently it damaged the performance of the ejector. This lesson will be very useful for the next design.

Another point which would deserve an improvement is the connection between evaporator exit and the ejector inlet. The pressure loss between the evaporator exit (measured in the close vicinity of the evaporator), and the measurement taken inside the diffuser (50 mm from the inlet) is due to a rather long path between these points, including two elbows and a "T" connection between secondary and primary flow lines. In order to improve the system performance, the connection between the evaporator and the suction port of the ejector must be as short and straight as possible.

The intermediate conditions, $T_{E\text{-}sat}$ = 5°C and $T_{E\text{-}sat}$ = 7.5°C, in both generator temperature conditions place themselves in between the two behaviours and are therefore omitted in Figs. 5-8. A comprehensive summary of all results is shown in Fig. 9, where the condenser critical temperature is plotted as a function of evaporator and generator conditions. Any point below each dotted line can be reached by the ejector in on-design operation.

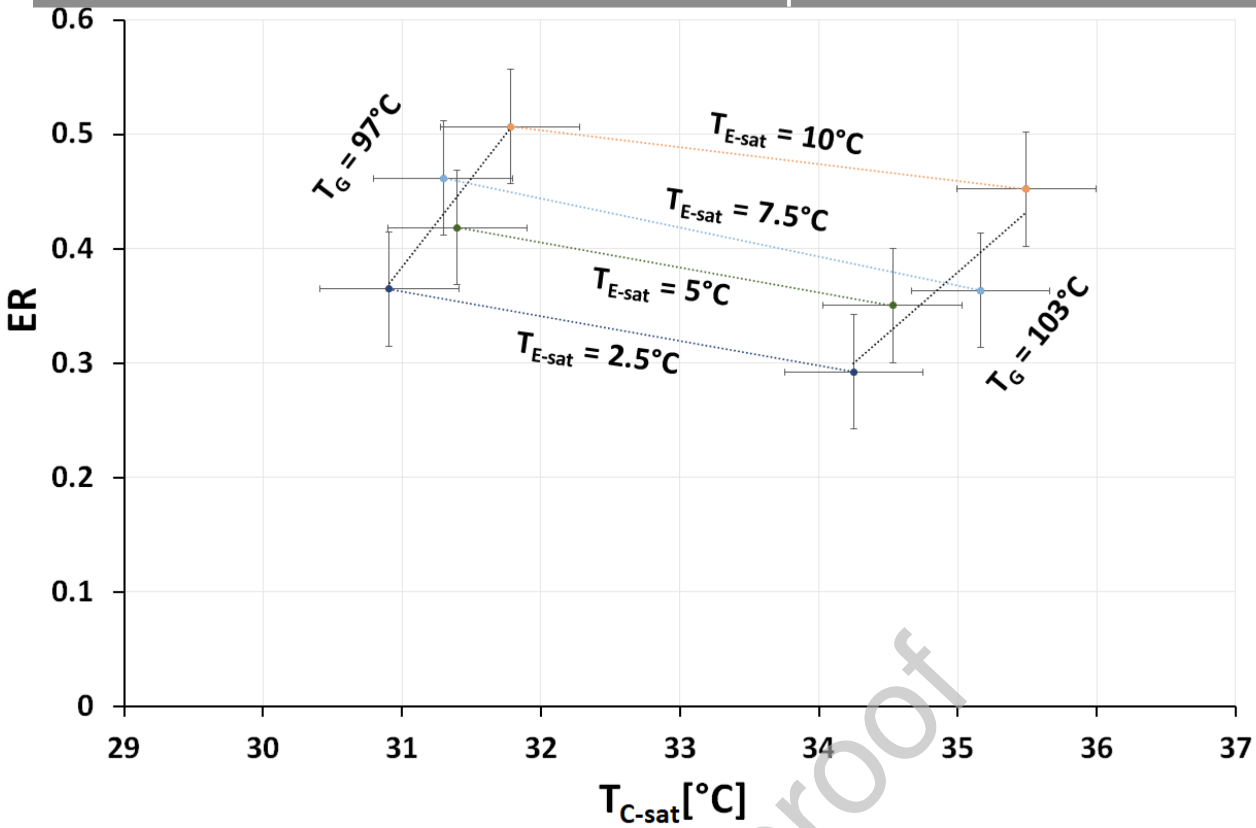

Figure 9 – Critical condenser temperature as a function of evaporator and generator saturation temperatures

As stated above, primary and secondary flow rates have been calculated from energy balances across the evaporator and the condenser. This decision was taken because direct measuring of the flow rates within the R1233zd(E) circuit is somewhat troublesome for various reasons:

- the fluid is saturated liquid or saturated vapour or two-phase;
- flow meters specifically calibrated for this fluids are difficult to find.

The energy balances may be written as:

$$\dot{m}_s = \dot{m}_{W-E}\frac{\Delta h_{W-E}}{\Delta h_E}$$

$$\dot{m}_m + \dot{m}_s = \dot{m}_{W-C}\frac{\Delta h_{W-C}}{\Delta h_C}$$

where subscript "*W*" refers to water and enthalpy differences Δh for R1233zd(E) are evaluated by NIST Refprop functions. As an example, at generator saturation temperature $T_{G\text{-sat}}$ = 103°C, $T_{E\text{-sat}}$ = 3.2°C and $T_{C\text{-sat}}$ = 34.3°C, the primary flow rate is $\dot{m}_m$ =5.082 kg/s and the secondary flow rate is $\dot{m}_s$ = 1.599 kg/s, yielding an entrainment ratio ER = 0.315.

The complete working cycle of the chiller has been modelled by simple thermodynamic calculations based on the experimental data and is shown in Fig. 10. All fluid properties are evaluated by NIST Refprop functions. Nozzle expansion line extends from point G fully outside of the two phase zone even if the starting point is saturated vapour, i.e. the ejector is completely free from condensation, thanks to the "dry expansion" featured by R1233zd(E).

However, as it comes out from the *Ts* diagram, the compression within the ejector is highly irreversible and brings the fluid at high temperature at point C. Correspondingly, the enthalpy increase is high. For a given energy input coming from the generator, this implies a reduction in the entrainment ratio and hence in the COP.

Note that R1233zd(E) allows a pressure at the generator that doesn't exceed 12 bar. This is a big advantage in terms of energy consumption and cost of the feed pump. For comparison, R1234ze(E) at 103°C would have a saturation pressure of 32 bar.

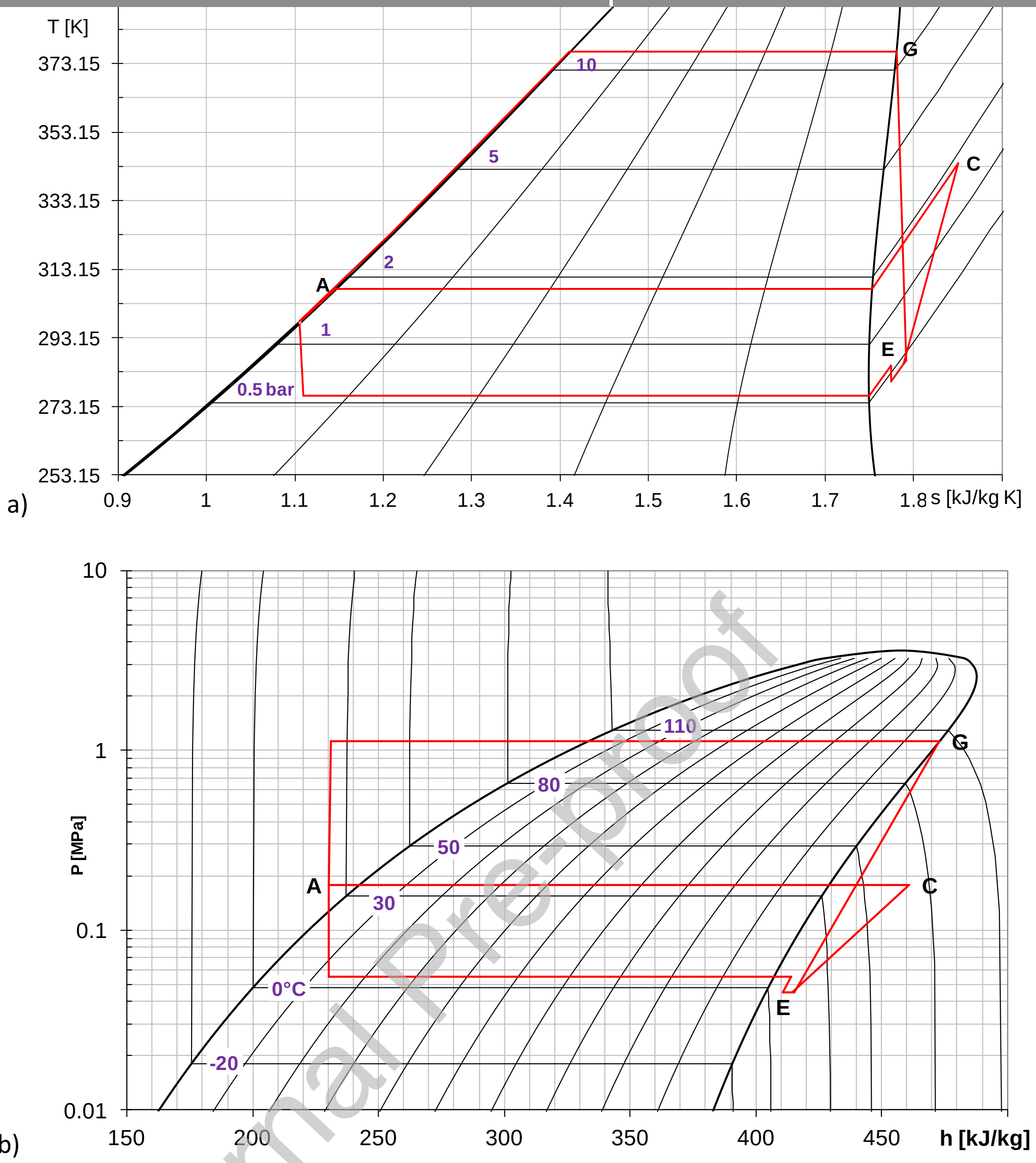

Figure 10 – Ts (a) and Ph (b) diagrams of the working cycle calculated on experimental data

4. Conclusions

This paper proves that an ejector chiller designed for R245fa can work efficiently with the low-GWP, non-flammable refrigerant R1233zd(E). A direct comparison of the results obtained with the two fluids is not possible, because the operating conditions that we have used in this work are different from those adopted in our previously published papers. The increased temperature at generator has inevitably caused a decrease in COP, but this loss has been largely compensated by the increased maximum discharge pressure.

The experimental results presented in this paper show that an ejector chiller designed according to the CRMC criterion has a good performance and a robust operation. When the ejector is operated at evaporator pressure near or above its design value, the transition across the critical discharge pressure is quite smooth and hence this operating limit may be overcome by limited amounts without great damage, apart from a performance decrease.

The full potential of the CRMC design is still unexploited. The experimental activity described in this paper shows that the design of the last part of the diffuser in our ejector is not producing any compression and must be modified.

The environmental safety of the R1233zd(E) needs to be proven in due course of time. Once this will be done, ejector chillers using this synthetic refrigerant may be an interesting alternative for LiBr absorption chillers, with a remarkable benefit in the capability to reach sub-zero temperatures. The system could work on waste heat in the temperature range commonly allowed by internal combustion engines and, if properly optimized, could be fit with an air-cooled condenser.

Wh [illegible] n. Synthetic refrigerants obviously have a much higher volumetric refrigeration capacity, and hence the size and cost of the system components is smaller. The cost of the refrigerant however is much higher, and may offset this result.

A second part of this paper will present some CFD results relying on the above-shown experimental data.

Acknowledgements

The research presented herein has received funding from the MIUR of Italy within the framework of PRIN2015 project «Clean Heating and Cooling Technologies for an Energy Efficient Smart Grid». A special thanks to Davide Refosco of Honeywell Performance Materials & Technologies for providing the fluid R1233zd(E).

Declaration of interests

The authors declare that they have no known competing financial interests or personal relationships that could have appeared to influence the work reported in this paper.

References

[1] M. Leblanc, Refrigerating machine, US patent 1029201, filed 1910, patented 1912.

[2] I. Eames, S. Aphornratana and D. Sun, "The jet-pump cycle a low cost refrigerator option powered by waste heat," *Heat Reco Syst CHP,* vol. 15, pp. 711-21, 1995.

[3] G. Grazzini, A. Milazzo and F. Mazzelli, Ejectors for Efficient Refrigeration, Springer, 2018.

[4] G. Besagni, R. Mereu and F. Inzoli, "Ejector refrigeration: A comprehensive review," *Renewable and Sustainable Energy Reviews ,* vol. 53 , p. 373–407, 2016.

[5] Z. Aidoun, K. Ameur, M. Falsafioon and M. Badache, "Current advances in ejector modelling, experimentation and applications for refrigeration and heat pump. Part1: Single phase ejectors," *Inventions,* vol. 4, no. 1, 2019.

[6] A. Little and S. Garimella, "A critical review linking ejector flow phenomena with component- and system-level performance," *International Journal of Refrigeration,* vol. 70, pp. 243-268, 2016.

[7] F. Mazzelli and A. Milazzo, "Performance analysis of a supersonic ejector cycle working with R245fa," *International Journal of Refrigeration,* vol. 49, pp. 79-92, 2015.

[8] J. Mahmoudian, A. Milazzo, I. Murmanskii and A. Rocchetti, "Experimental results from R245fa chiller," in *Heat powered Cycles*, Bayreuth, Germany, 2018.

[9] K. Shestopalov, B. Huang, V. Petrenko and O. Volovyk, "Investigation of experimental ejector refrigeration machine operating with refrigeratnt R245fa at design and off-design working condition. Part1: Theoretical analysis," *internation journal of refrigeration,* vol. 29, pp. 201-211, 2015.

[10] K. Shestopalov, B. Huang, V. Petrenko and O. Volovyk, "Investigation of an experimental ejector refrigeration machine operating with refrigerant R245fa at design and off-design working conditions. Part2: Theoretical and experimental results," *International journal of refrigeration,* vol. 55, pp. 212-223, 2015.

[11] E. Narimani, M. Sorin, P. Micheau and H. Nesreddine, "Dynamic modeling of an R245fa ejector based refrigeration system," *International journal of refrigeration,* 2019.

[12] M. Bencharif, S. Poncet, H. Nesreddine and S. Zid, "Droplet injection at the diffuser outlet in an ejector-based refrigeration cycle working with R245fa," in *25th IIR international congress of refrigeration*, Montréa, Canada, 2019.

[13] M. Milazzo and A. Rocchetti, "Modelling of ejector chillers with steam and other working fluids," *International Journal of Refrigeration,* vol. 57, pp. 277-287, 2015.

[14] J. M.Calm, "The next generation of refrigerants - historical review, consideration, and outlook," *International journal of refrigeration,* vol. 31, no. 7, pp. 1123-1133, 2008.

[15] S. Eyerer, F. Dawo, J. Kaindl, C. Wieland and H. Spliethoff, "Experimental investigation of modern ORC working fluids R1224zy(Z) and R1233zs(E) as replacemnets for R245fa," *Applier energu journal,* vol. 240, pp. 946-963, 2019.

[16] [illegible] "Simultaneous experimental comparison of low-GWP refrigerants as drop-in replacemnets to R245fa for Organic Rankine cycle application: R1234ze(Z), R1233zd(E) and R1336mzz(E)," *Energy,* vol. 173, pp. 721-731, 2019.

[17] J. Mahmoudian, F. Mazzelli, A. Milazzo and A. Rocchetti, "Experiemntal and numerical activity on a prototype ejector chiller," in *37th UIT Heat transfer conference* , Padova, 2019.

[18] I. Eames, "A new prescription for the design of supersonic jet-pumps: the constant rate of momentum change method," *Applied Thermal Engineering,* vol. 22, p. 121–31, 2002.

[19] I. Eames, A. Ablwaifa and V. Petrenko, "Results of an experimental study of an advanced jet-pump refrigerator operating with R245fa," *Applied Thermal Engineering,* vol. 27, pp. 2833-284, 2007.

[20] B. Kittratana, S. Aphornratana, T. Thongtip and N. Ruantrakoon, "Comaprison of traditional and CRMC ejector performance used in steam ejector refrigeration," *Energy procedia,* vol. 138, pp. 476-481, 2017.

[21] A. Milazzo, A. Rocchetti and I. Eames, "Theoretical and experimental activity on Ejector Refrigeration," *Energy Procedia ,* vol. 45 , p. 1245 – 1254, 2014 .

[22] R. Figliola and D. Beasley, Theory and design for mechanical measurements, 3rd edition, Hoboken, NJ: John Wiley & Sons Inc, 2000.

[23] R. Moffat, "Describing the uncertainties in experimental results," *Experimental thermal and fluid science,* vol. 1, pp. 3-17, 1988.

[24] *NIST REFPROP, Reference Fluid Thermodynamic and Transport Properties Database, version 9.1,* 2018.